

A ROBUST DAMPING CONTROLLER FOR AN HV–ACDC SYSTEM USING A LOOP–SHAPING PROCEDURE

Abu H. M. A. Rahim^{*} — Edwin P. Nowicki^{**}

The design of a robust damping controller in the thyristor converter circuit of a high voltage ACDC link in a power system has been presented. The H_∞ -based design has been realized through a relatively new graphical design procedure termed the 'loop-shaping' technique. A detailed power system model including the dynamics of the generator, exciter, HVDC link and converter controllers has been considered. The robust controller is tested for a number of operating conditions considering various disturbances on a power system. The robust rectifier controller has been shown to provide excellent damping characteristics over a wide range of operation.

Key words: HVDC link, HV-ACDC, damping control, power system stability, robust control, loop-shaping

1 INTRODUCTION

High voltage DC (HVDC) transmission technology, based on new and powerful semiconductor devices, offers technical and economic benefits such as: lower line costs, no need for common frequency control, stable operation even with low-power interconnection, improved dynamic conditions in the ac systems *etc.* While a double circuit ac line can render one of the interconnected systems unstable in the event of a severe fault, inclusion of a parallel HVDC bi-pole can provide stable operating conditions. Using its fast control potential, the HVDC system can efficiently damp stability oscillations [1]. To obtain adequate control, operation at higher than normal rectifier firing angles or higher than minimum inverter extinction angles may be required [2].

The stability and control aspect of an HVDC link has been a matter of intensive research over a number of years. HVDC control signals are required to provide adequate synchronizing and damping torque at generators, and to insure voltage stability. Since HVDC transmission results in active and reactive power injections at two or more locations separated by hundreds of kilometers, controls must be robust so that unfavourable modal interactions and voltage stabilities are avoided [2]. Control design for the non-linear generator and also modelling of the interaction between ac and dc regions are often done through small signal analysis [3, 4]. Since small signal models only predict stability in a small operating range, the variations in rectifier side ac system parameters can cause oscillatory instabilities with frequencies around first harmonic. Through simple modelling, reference [5] demonstrated that the tie-line power modulation of both ac and dc links can stabilize frequency oscillations in the ac system. Hammad [6] demonstrated that a

HVDC scheme fitted with classical constant power control increases the risk for transient rotor angle and voltage instabilities because it deprives the much-needed synchronizing torque to the ac system during disturbances. However, large signal stabilizing control strategies can produce large amount of synchronizing and damping torques effectively stabilizing the ac system.

One important factor in control design for stability studies is the extent of dynamic modelling. A detailed model used in dynamic and transient stability studies represents the electromagnetic effects of the HVDC transmission and the high frequency dynamics of the pole control. However, a pseudo-steady-state dynamic HVDC model used in such studies considers almost instantaneous converter operations. These may not reflect the exact dynamic interactions [7]. Damping control design should, however, include the L/R converter dynamics in addition to reasonably smaller generator time constants. Global optimal designs for HVDC systems have been reported which employ artificial intelligence based techniques [8]. Robust control designs have also been reported in the literature in the recent times [9, 10]. The controls for AVR, converter, governor, *etc.* have been derived through the Riccati matrix of the linearized system equations employing identification and rule based system in [9]. The robustness measures are only implicitly incorporated in these studies.

Excellent and inexpensive software are available today for control design purposes. However, their efficient use depends heavily on practical design experience gained by hand or graphical calculations. For instance, the QFT-Matlab toolbox is used to solve highly uncertain plant feed back problems in the frequency domain. However, this software can never be used efficiently unless the designer has experience on how to deal with bounds on the

^{*} Department of Electrical Engineering King Fahd University of Petroleum & Minerals Dhahran, Saudi Arabia, mailing address: KFUPM, Box 349, Dhahran 31261, Saudi Arabia, E-mail: abrahim@kfupm.edu.sa

^{**} Department of Electrical Engineering University of Calgary, Calgary, AB, Canada

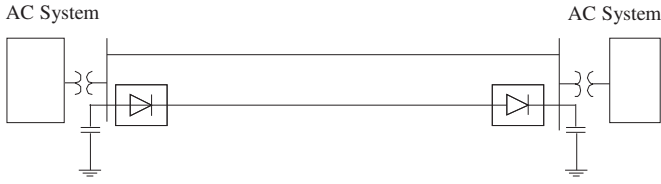


Fig. 1. Parallel AC-DC link between two AC systems.

nominal open-loop transmission function in the logarithmic complex plane. Of special interest are the gain bandwidth limitations when plant to be controlled is not minimum phase, but rather contains unstable poles, and/or right-half-plane zeroes [10]. The robust control design for a power system problem which is highly uncertain and which also may be on the threshold of instability is, generally, difficult. The H_∞ based strategies often involve complicated minimization procedures and may not provide a constant parameter controller for such cases [11].

This article presents a robust damping controller design for the HVDC link in a power system. The design employs the H_∞ robustness measures, and the controller is realized through a supervised 'loop-shaping' procedure [12]. Simulation results demonstrate that the controller designed damps the electromechanical oscillations in the power system very effectively for a wide range of operating conditions.

2 HIGH VOLTAGE ACDC SYSTEM MODEL

Figure 1 shows two ac systems connected through a transmission line in parallel with a two terminal dc link. For simulation purposes, the ac system on the left is replaced by an equivalent generator. The ac system on the right side may be considered as the large power pool. The generator is considered to be equipped with a static excitation system. The generator-exciter is represented as a 6th order state model. The equations are included in the Appendix.

The dc link and converter regulator equations are given in the following:

$$\begin{aligned} V_{dr} &= V_{sr} \cos \alpha - \frac{\pi}{6} x_{cr} I_{dc}, \\ V_{di} &= V_{si} \cos \gamma - \frac{\pi}{6} x_{ci} I_{dc}. \end{aligned} \quad (1)$$

The dc line equation is

$$V_{dr} = r_1 I_{dc} + \frac{x_1}{\omega_0} \dot{I}_{dc} + V_{di}. \quad (2)$$

The converter current regulator equations are

$$\begin{aligned} \Delta \alpha &= \frac{K_r}{1 + sT_r} [I_{ds} - I_{dc} + u_1], \\ \Delta \gamma &= \frac{K_r}{1 + sT_i} [I_{ds} - I_{mar} - I_{dc} + u_2]. \end{aligned} \quad (3)$$

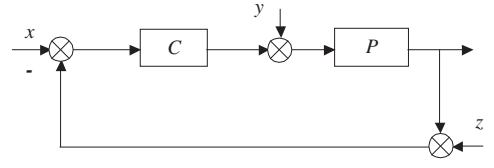


Fig. 2. The controller configuration.

Here, V_{dr} , V_{di} , V_{sr} , V_{si} stand for the dc and ac voltages on the rectifier and inverter sides, respectively; I_{dc} is the dc current, I_{ds} is the dc current setting; u_1 and u_2 are the converter firing angle controls, respectively. The single bridge dc link configuration used in this analysis is shown in the Appendix. Combining the six differential equations for the ac system and the three from the dc line and the converters, and after some algebraic manipulation we can obtain the following 9th order state model,

$$\dot{\mathbf{x}} = \mathbf{f}(\mathbf{x}, \mathbf{u}). \quad (4)$$

Linearizing (4) around a nominal operating point yields

$$\begin{aligned} \dot{\mathbf{x}} &= \mathbf{A}\mathbf{x} + \mathbf{B}\mathbf{u}, \\ \mathbf{y} &= \mathbf{H}\mathbf{x}. \end{aligned} \quad (5)$$

The linearized states are the variations of the original quantities and \mathbf{y} is the selected output variable.

3 ROBUST CONTROL DESIGN

The damping control problem for the non-linear power system model is stated as: given the non-linear set of equations (4), design a controller whose output \mathbf{u} will stabilize the system oscillations following a perturbation. Since there is no general method of designing a stabilizing controller for the non-linear system, one way would be to perform the control design for the linearized system, the linearization being carried out around a nominal operating condition. If the controller designed is 'robust' enough to perform well for the other operating conditions in around the nominal one, the design objectives are met.

The changes in operating points of the non-linear system can be considered as changes in the coefficients of the \mathbf{A} and \mathbf{B} matrices in (5). These perturbations are modelled as multiplicative uncertainties and robust design procedure is applied to the nominal system subjected to these uncertainties. This section gives a brief theory of the uncertainty modelling, the robust stability and performance criteria and a graphical design technique termed loop-shaping, which is employed to design the robust controller. Finally, the algorithm for the control design is presented.

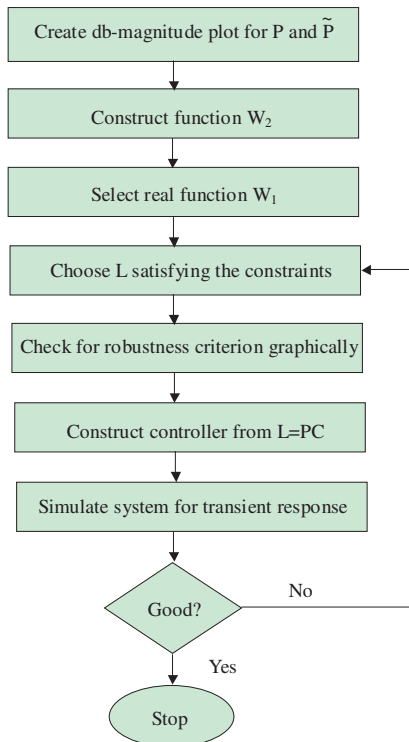


Fig. 3. The design flow chart.

Uncertainty Modelling and Robust Stability

Suppose that a plant having a nominal transfer function $G = \mathbf{H}[s\mathbf{I} - \mathbf{A}]^{-1}\mathbf{B}$ belongs to a bounded set \mathbf{G} . Consider that the perturbed transfer function resulting from the variations in operating conditions, can be expressed in the form

$$\tilde{G} = (1 + \Omega W_2)G. \quad (6)$$

Here, W_2 is a fixed stable transfer function, also called the weight, and Ω is a variable transfer function satisfying $\|\Omega\|_\infty < 1$. The infinity norm (∞ -norm) of a function is the least upper bound of its absolute value, also written as $\|\Omega\|_\infty = \sup_\omega |\Omega(j\omega)|$, is the largest value of gain on a Bode magnitude plot [12, 14].

In the multiplicative uncertainty model (6), ΩW_2 is the normalized plant perturbation away from 1. If $\|\Omega\|_\infty < 1$, then

$$\left| \frac{\tilde{G}(j\omega)}{G(j\omega)} - 1 \right| \leq |W_2(j\omega)|, \quad \forall \omega. \quad (7)$$

So, $|W_2(j\omega)|$ provides the uncertainty profile, and in the frequency plane is the upper boundary of all the normalized plant transfer functions away from 1.

Consider a multi-input control system given in Fig. 2. A controller C provides robust stability if it provides internal stability for every plant in the uncertainty set \mathbf{G} . If L denotes the open-loop transfer function ($L = PC$), then the sensitivity function S is written as

$$S = \frac{1}{1 + L}. \quad (8)$$

The complimentary sensitivity function, or the input-output transfer function is

$$T = 1 - S = \frac{PC}{1 + PC}. \quad (9)$$

For a multiplicative perturbation model [12, 15], robust stability condition is met if and only if $\|W_2 T\|_\infty < 1$. This implies that

$$|\Omega(j\omega)W_2(j\omega)L(j\omega)| < |1 + L(j\omega)|, \quad \forall \omega; \quad \text{and } \|\Omega\|_\infty < 1. \quad (10)$$

The maximum loop gain, $\| -W_2 T \|_\infty$ is less than one for all allowable Ω , if and only if the small gain condition $\|W_2 T\|_\infty < 1$ holds. The nominal performance condition for an internally stable system is given as $\|W_1 S\|_\infty < 1$, where W_1 is a real-rational, stable, minimum phase transfer function, also called a weighting function. If G is perturbed to $\tilde{G} = (1 + \Omega W_2)G$, S is perturbed to

$$\tilde{S} = \frac{S}{1 + \Omega W_2 T}. \quad (11)$$

The robust performance condition should therefore be

$$\|W_2 T\|_\infty < 1, \quad \text{and } \left\| \frac{W_1 S}{1 + \Omega W_2 T} \right\| < 1, \quad \forall \|\Omega\| < 1. \quad (12)$$

Combining all the above, it can be shown that a necessary and a sufficient condition for robust performance is

$$\| |W_1 S| + |W_2 T| \|_\infty < 1. \quad (13)$$

Loop Shaping Technique and the Algorithm

Loop shaping is a graphical procedure to design a proper controller C satisfying the robust stability and performance criteria given above. The basic idea of the method is to construct the loop transfer function L to satisfy the robust performance criterion approximately, and then to obtain the controller from the relationship $C = L/P$. Internal stability of the plants and properness of C constitute the constraints of the method. A condition on L is that PC should not have any pole zero cancellation.

A necessary condition for robustness is that either or both $|W_1|$, $|W_2|$ must be less than one [12]. If a monotonically decreasing W_1 satisfying the other constraints is selected, it can be shown that at low frequency the open-loop transfer function L should satisfy

$$|L| > \frac{|W_1|}{1 - |W_2|} \quad (14)$$

while, for high frequency

$$|L| < \frac{1 - |W_1|}{|W_2|} \approx \frac{1}{|W_2|}. \quad (15)$$

At high frequency $|L|$ should roll-off at least as quickly as $|P|$ does. This ensures properness of C . The general features of the open loop transfer function is that the gain at low frequency should be large enough, and $|L|$ should not drop-off too quickly near the crossover frequency, thus assuring internal instability. The algorithm to generate a control transfer function C is represented in the following flow chart (Fig. 3).

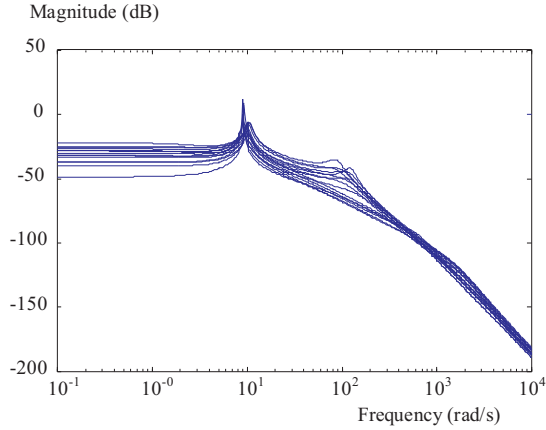


Fig. 4. Bode magnitude diagram of nominal and perturbed plant functions.

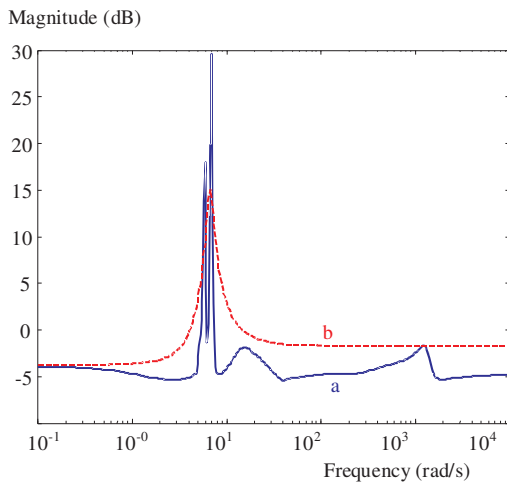


Fig. 5. The weighting function W_2 from frequency response profiles of Fig. 3, (a) W_2 , (b) $\sup|\tilde{G}(j\omega)/G_{nom}(j\omega) - 1|$.

4 ROBUST DESIGN IMPLEMENTATION

The high voltage ACDC system transfer function G , between the rectifier converter input and the generator speed deviation output, for nominal generator power output of 1 pu at 0.95 lagging power factor is obtained as,

$$G = [-266s(s + 2528.329)(s + 179.122)(s + 13.0209) \times (s + 9.896)(s + 3.69)] / [(s + 0.9577)(s + 4.66)(s + 10) \times (s + 16.044)(s + 98.869)(s^2 + 0.1282s + 35.97) \times (s^2 + 537.44s + 1.932e6)]. \quad (16)$$

Off-nominal power output in the range of 0.3–1.4 pu and power factor of up to 0.8 lag/lead which gave steady state stable situations were considered in the robust design. The log-magnitude vs. frequency plots for the nominal and perturbed plants are shown in Fig. 4. Data for the HV-ACDC system has been taken from [13].

The quantity $|\tilde{G}(j\omega)/G_{nom}(j\omega) - 1|$ is constructed for each perturbed plant $\tilde{G}(j\omega)$ and the upper envelope in

the frequency plane is fitted to the function W_2 as shown in Fig. 5,

$$W_2(s) = \frac{0.6581s^2 + 4.68s + 23.4}{0.8s^2 + 0.84s + 36}. \quad (17)$$

A Butterworth filter, which satisfies the properties of $W_1(s)$, is selected as

$$W_1(s) = \frac{K_c f_c^2}{s^3 + 2s^2 f_c + 2s f_c^2 + f_c^3}. \quad (18)$$

Values of $K_c = 0.1$ and $f_c = 1$ were observed to satisfy the requirement on the open loop transfer function L . For W_1 and W_2 selected above, the open-loop transfer function is chosen by trial and error to satisfy all the frequency response constraints on it. Figure 6 shows the magnitude plots of L and the boundary functions (14) and (15). The controller transfer function is then obtained through the relation $L = GC$ and is given as

$$C = \frac{200(s + 0.1)(s + 0.9597)(s + 2)}{s(s + 0.01)(s + 3.69)}. \quad (19)$$

The robust and nominal performance measures (12) and (13) are shown in Fig. 7. It can be observed that the nominal performance measure is much below 0 db. The robust stability measure is marginally violated at the corner frequency. This is for a worst-case design in the absence of a damping term in the electromechanical swing equation.

While selecting the open-loop transfer function, the internal stability of the plant in addition to design criterion (12)–(14) should be checked. A disturbance of 100% input torque pulse for 0.05 second on the generator shaft was simulated for this purpose. The variations of the generator for the nominal operating point with and without the robust controller are plotted in Fig. 8. It can be seen that the response without any control is very poorly damped, but the proposed robust controller eliminates the oscillations completely in less than a second. While it is possible to obtain still better damping by adjusting the open-loop gain function L , this could drive the firing angle to unacceptable levels.

The controller designed was then tested for operation on a number of operating conditions for various disturbances in the power output range of 0.3–1.4 pu. The rotor angle characteristics for four cases are given in Fig. 9. The results presented are for a) a 100% torque pulse for 0.05 second when the generator is loaded to 1.3 pu power output at 0.85 lagging power factor, b) a three-phase fault on the remote bus cleared after 4 cycles, the generator being loaded at nominal load of 1 pu power output, c) 100% torque pulse disturbance at nominal loading, and d) 0.6 pu loading at 0.83 lagging power factor. The corresponding terminal voltage variations for the 4 cases are shown in Fig. 10. As can be observed, the robust controller provides extremely good damping to the system oscillations for all the operating conditions and for various disturbance conditions. The electrical transients, as depicted by the terminal voltage characteristics, have also been controlled very effectively.

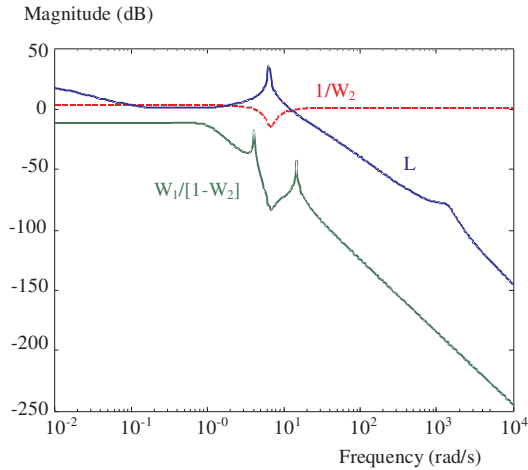


Fig. 6. The loop-shaping boundary plots.

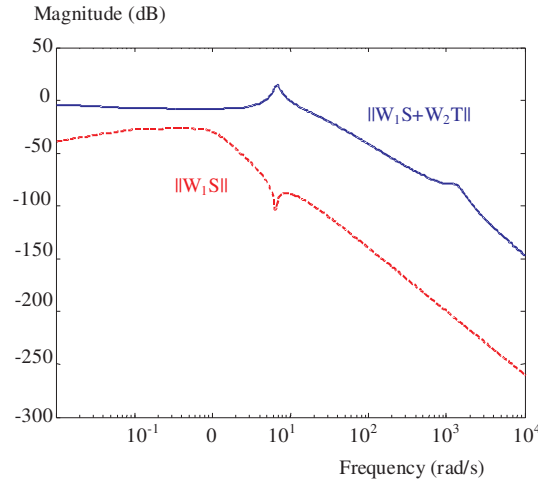


Fig. 7. Plot of nominal and robust performance indices.

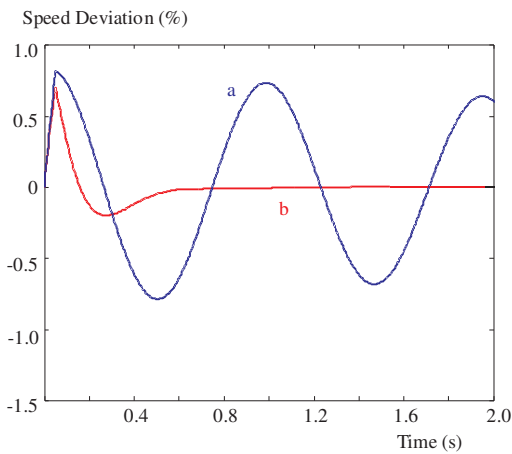


Fig. 8. Generator angular speed variation following a 100% input torque pulse for 0.05 sec with, (a) no control, (b) proposed robust damping controller.

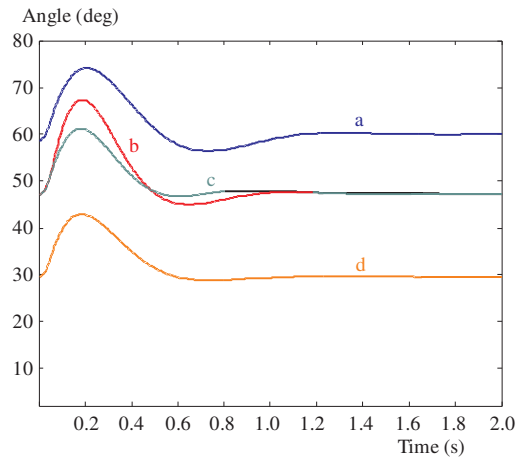


Fig. 9. Rotor angle characteristics with the robust damping controller for (a) 1.3 pu output and 100% torque pulse (b) nominal power output with three-phase fault (c) nominal power output and torque pulse disturbance, and (d) 0.6 pu power output with torque pulse disturbance.

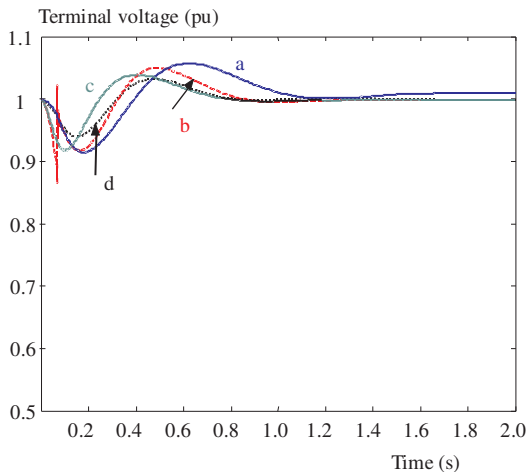


Fig. 10. Terminal voltage variations corresponding to Fig. 9.

5 CONCLUSIONS

A robust converter control for damping the transients in a high voltage ACDC power system has been proposed. The design is carried out retaining all the important ac system dynamics as well as those of the relatively

short dc link and dc controller time constants. Simulation studies considering a number of disturbance conditions show that the controller designed provides excellent damping properties over a wide range of operating conditions for the high voltage ACDC system.

The robust design procedure involves a simple graphical loop-shaping construction technique avoiding complex minimization procedures normally encountered in such problems. The design produces a fixed parameter controller making its realization straightforward.

APPENDIX

The electromechanical swing equation is

$$\frac{2H}{\omega_0} \ddot{\delta} = T_m - T_e, \tag{A1}$$

T_m is the mechanical input torque, and the electrical output torque is expressed as,

$$T_e = \psi_d i_q - \psi_q i_d. \tag{A2}$$

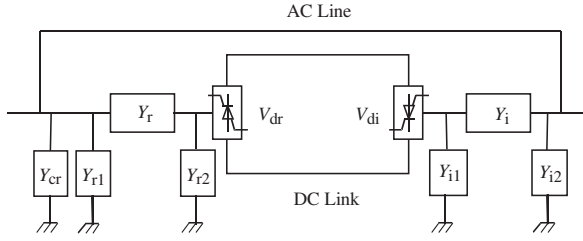


Fig. 11. Circuit diagram of a single bridge HVDC link.

The flux linkage relations are

$$\begin{bmatrix} \psi_d \\ \psi_q \\ \psi_{fd} \end{bmatrix} = \begin{bmatrix} -x_d & 0 & x_{afd} \\ 0 & -x_q & 0 \\ -x_{afd} & 0 & x_{ffd} \end{bmatrix} \begin{bmatrix} i_d \\ i_q \\ i_{fd} \end{bmatrix}. \quad (\text{A3})$$

The terminal voltage of the generator at the transformer end along d - q axes are,

$$\begin{aligned} v_d &= -r_a i_d + \frac{\omega}{\omega_0} \psi_q + \frac{1}{\omega_0} \dot{\psi}_d + i_q x_t, \\ v_q &= -r_a i_q + \frac{\omega}{\omega_0} \psi_d + \frac{1}{\omega_0} \dot{\psi}_q - i_d x_t. \end{aligned} \quad (\text{A4})$$

The voltage equations for the ac line are,

$$\begin{aligned} v_d &= -r_e i_{ld} - \frac{\omega}{\omega_0} x_e i_{lq} + v_{bd}, \\ v_q &= -r_e i_{lq} + \frac{\omega}{\omega_0} x_e i_{ld} + v_{bq}. \end{aligned} \quad (\text{A5})$$

The excitation system is represented through the equation,

$$E_{fd} = \frac{K_E}{1 + sT_E} [v_{tr} - v_t + u_E], \quad (\text{A6})$$

u_E is the excitation system control. The details of these equations are given in [12].

The Π -networks in the left and right side represent the rectifier and inverter transformers in HVDC link. Y_{cr} is the susceptive admittance of the capacitor on the rectifier side. A similar capacitor may be included in the inverter side.

Acknowledgement

The authors wish to acknowledge the facilities provided at the King Fahd University of Petroleum & Minerals towards this research.

REFERENCES

- [1] POVH, D. : Use of HVDC and FACTS, Proceedings of the IEEE **88** No. 2 (2000), 235–245.
- [2] IEEE Special Stability Controls Working Group, HVDC Controls for Dynamic Performance, IEEE Trans. on Power Systems **6** No. 2 (1991), 743–752.

- [3] JAVOCIC, D.—PATHALAWATHA, N.—ZAVAHIR, M. : Analytical Modelling of HVDC-HVAC Systems, IEEE Trans. on Power Delivery **14** No. 2 (1999), 506–511.
- [4] JAVOCIC, D.—PATHALAWATHA, N.—ZAVAHIR, M. : Small Signal Analysis of HVDC-HVAC Interaction, IEEE Trans. on Power Delivery **14** No. 2 (1999), 525–530.
- [5] NGAMROO, I. : A Stabilization of Frequency Oscillations using a Power Modulation Control of HVDC Link in a Parallel AC-DC Interconnected System, Proc. Power Conversion Conference, PCC Osaka 2000, pp. 1405–1410.
- [6] HAMMAD, A. E. : Stability and Control of HVDC and AC Transmission in Parallel, IEEE Trans. on Power Delivery **14** No. 4 (1999), 1545–1554.
- [7] JOHNSON, B. K. : HVDC in Stability Studies, IEEE Trans. on Power Delivery **4** No. 2 (1989), 1153–1163.
- [8] WANG, Y. P.—HUHR, D. R.—CHUNG, H. H.—WATSON, N. R.—ARRILAGA, J.—MATAIR, S. S. : Design of an Optimal PID Controller in AC-DC Power System Using Modified Genetic Algorithm, Proc. Int. Conf. on Power System Tech., POWERCON 2000, pp. 1437–1442.
- [9] TO, K. W. V.—DAVID, A. K.—HAMMAD, A. E. : A Robust Co-ordinated Control Scheme for HVDC Transmission with Parallel AC Systems, IEEE Trans. on Power Delivery **9** No. 3 (1994), 1710–1716.
- [10] SIDI, V. : Design of Robust Control Systems – From Classical to Modern Practical Approaches, Krieger Publishing Company, Florida, USA, 2001.
- [11] VEMKATARAMAN, S.—KHAMMASH, M. H.—VITTAL, V. : Analysis and Synthesis of HVDC Controls for Robust Stability of Power Systems, IEEE Trans. on Power Systems **10** No. 4 (1995), 1933–1938.
- [12] DOYLE, J. C.—FRANCIS, B. A.—TANNENBAUM, A. R. : Feedback Control Theory, MacMillan Publishing Co, New York, 1992.
- [13] RAHIM, A. H. M. A.—EL-AMIN, I. M. : Stabilization of a High Voltage ACDC Power System I. Evaluation of Control Strategies, IEEE Trans Power App. and Systems **104** No. 11 (1985), 3084–3091.
- [14] CHAO, A.—ATHANS, M. : Stability Robustness to Unstructured Uncertainty for Linear Time Invariant Systems, The Control Handbook (W.S. Levine, ed.), CRC Press and IEEE Press, 1996.
- [15] DAHLEH, M. A. : l_1 Robust Control: Theory, Computation and Design, The Control Handbook (W.S. Levine, ed.), CRC Press and IEEE Press, 1996.

Received 29 March 2004

Abu H. M. A. Rahim (Professor) received his PhD from the University of Alberta, Edmonton, Canada in 1972. After a brief post-doctoral work at the University of Alberta, he rejoined the faculty in the Bangladesh University of Engineering, Dhaka. Dr. Rahim then worked at the University of Strathclyde, Glasgow (U.K.) and the University of Bahrain. Presently, Dr. Rahim is a Professor of Electrical Engineering at the K.F. University of Petroleum and Minerals, Saudi Arabia. His main fields of interest are power systems control and artificial intelligence. Dr. Rahim is a senior member of IEEE (USA) and Fellow of the Institute of Engineers, Bangladesh.

Edwin P. Nowicki (Dr) received his PhD from University of Toronto in 1991. He worked at Inverter Controls Ltd., Burlington, Ontario in the area of medium voltage induction motor drives before joining the University of Calgary in 1992, where he is presently an Associate Professor in the Department of Electrical and Computer Engineering. His current research projects include fuzzy logic controls and artificial neural networks to power electronic devices.